

Numerical Analysis of two Quantum Systems in the Path Integral Formulation via MCMC Methods

ULYANA DUPLETSA

University of Milan - Bicocca

Abstract

The path integral formulation is a useful mathematical tool largely used in quantum field theory. For most systems it is impossible to evaluate it analytically, so numerical methods are needed, such as the Monte Carlo ones. In this work we will make use of Markov Chain Monte Carlo (MCMC) algorithms for two different systems: the quantum harmonic oscillator and the scalar $\lambda\phi^4$ theory.

In the first part, we implement a Metropolis algorithm to simulate one dimensional trajectories for a quantum harmonic oscillator with periodic boundary conditions. This system has an analytic solution and thus allows us to test our program comparing the numerical results with the theoretical ones.

In the second part, the $\lambda\phi^4$ model on the cubic lattice in three dimensions is studied. The local updates used in the previous section become inefficient and a global algorithm, called Hamiltonian Monte Carlo, is implemented. It proposes new configurations by solving the molecular dynamics equations via the leapfrog integration method, to which a final Metropolis step is added. As a consequence the HMC algorithm becomes exact with high acceptance rate, time-reversibility and area-preserving properties. The field configurations are used then to calculate observables for the study of the spontaneous symmetry breaking, varying both a parameter of the action and the lattice size.

CONTENTS

I	Introduction to the Path Integral	3
i	Evolution operator in quantum mechanics	3
ii	Interpretation and properties of \hat{G}	5
	ii.1 Transfer operator	6
	ii.2 Analytic continuation to the Euclidean propagator	7
	ii.3 Back to Minkowski	8
	ii.4 Physical meaning of the path integral formalism	9
iii	Connection with statistical mechanics: partition function and numerical methods	9
iv	Outline of the project	11

CONTENTS

II Numerical Methods: MCMC	12
i Markov Chain Monte Carlo (MCMC)	12
ii Ergodic theorem and asymptotic distribution	12
III Metropolis Monte Carlo: harmonic oscillator	14
i Harmonic oscillator in 1-D	14
ii Metropolis algorithm	16
ii.1 Thermalization: reaching equilibrium	16
ii.2 Correlation function	16
ii.3 Autocorrelation function: how to uncorrelate data	17
iii $\Delta\epsilon$ and matrix element: results vs theoretical predictions	20
IV Hamiltonian Monte Carlo (HMC): $\lambda\phi^4$ theory	23
i Scalar $\lambda\phi^4$ theory on lattice in 3-D	23
ii Hamiltonian Monte Carlo (HMC)	23
ii.1 Sampling random momenta π	26
ii.2 Discrete MD integrator: Leapfrog	26
ii.3 Time-Reversibility and Area-Preserving	27
ii.4 The hamiltonian is not conserved	27
ii.5 The accept/reject step	27
iii Spontaneous symmetry breaking	29
A Jackknife method for error analysis	32
A Outline of the programs	34
i Harmonic oscillator (LFC18)	34
ii $\lambda\phi^4$ theory (phi4)	35

I. INTRODUCTION TO THE PATH INTEGRAL

I. EVOLUTION OPERATOR IN QUANTUM MECHANICS

We want to formulate the path integral for a quantum system in one dimension. The starting point is the quantum evolution operator, which has to be evolved over a discretized time and then the limit at continuum should be taken.

We have to consider that the evolution of a quantum system can be described using both the Heisenberg and the Schroedinger pictures.

In the *Schroedinger picture*, the operators, which we generally denote with \hat{O}_S , do not evolve in time, whereas the states, denoted with $|x, t\rangle_S$, do evolve according to the Schroedinger equation

$$i\frac{\partial}{\partial t}|x, t\rangle_S = \hat{H}|x, t\rangle_S$$

where \hat{H} is the Hamiltonian operator given by

$$\hat{H} = \frac{\hat{p}^2}{2m} + V(\hat{x})$$

Therefore

$$|x, t\rangle = e^{-i\hat{H}(t-t_0)}|x, t_0\rangle, \quad t > t_0$$

In the *Heisenberg picture*, instead, the operators depend on time $\hat{O}_H(t)$ and the states $|x\rangle_H$ do not. In this case the evolution equation is for operators and it is given by

$$i\frac{\partial}{\partial t}\hat{O}_H(t) = [\hat{O}_H, \hat{H}]$$

Therefore

$$\hat{O}_H(t) = e^{i\hat{H}t}\hat{O}_H(0)e^{-i\hat{H}t}$$

The two formalisms are equivalent if we set

$$|x\rangle_H = |x, t=0\rangle_S, \quad \hat{O}_H(0) = \hat{O}_S$$

Then the following equality holds

$${}_S\langle x, t|\hat{O}_S|x, t\rangle_S = {}_H\langle x|\hat{O}_H(t)|x\rangle_H$$

Whatever is the picture we are working in, all the dynamics is encoded within the retarded propagator

$$\hat{G}(t, t_0) \equiv \theta(t - t_0)e^{-i\hat{H}(t-t_0)} \tag{1}$$

where θ is the Heaviside step function. (1) satisfies the following differential equation

$$\begin{cases} i\frac{\partial}{\partial t}\hat{G}(t, t_0) = \hat{H}\hat{G}(t, t_0) + i\delta(t - t_0)\hat{\mathbb{1}} \\ \hat{G}(t, t_0)|_{t=t_0} = \hat{\mathbb{1}} \end{cases} \quad (2)$$

The \hat{H} operator has the following eigenstates and eigenvalues

$$\hat{H}E_n = E_n|E_n\rangle, \quad u_n(x) = \langle x|E_n\rangle \quad (3)$$

where n is the set of indexes (eventually continuous) that identifies the eigenstates.

Then, remembering that $\hat{\mathbb{1}} = \sum_n |E_n\rangle\langle E_n|$, we can rewrite the retarded propagator as

$$\hat{G}(t, t_0) = \theta(t - t_0) \sum_n e^{-iE_n(t-t_0)} |E_n\rangle\langle E_n| \quad (4)$$

After performing the Fourier transform

$$\tilde{G}(z) = \int_{-\infty}^{+\infty} dt \left[e^{iz(t-t_0)} \hat{G}(t, t_0) \right] = \int_0^{+\infty} dt \left[e^{iz(t-t_0)} e^{-i\hat{H}(t-t_0)} \right], \quad \text{for } t_0 \geq 0 \quad (5)$$

The integral (5) is well defined and convergent if $Im(z) > 0$. Then it can be written as

$$\tilde{G}(z) = \frac{1}{z - \hat{H}} = i \sum_n \frac{1}{z - E_n} |E_n\rangle\langle E_n| \quad (6)$$

On the remaining part of the complex plane, $\tilde{G}(z)$ is the analytic continuation of (6).

If we define

$$\hat{G}(x, t; x_0, t_0) \equiv \langle x | \hat{G}(t, t_0) | x_0 \rangle \quad (7)$$

then, using (3) and (4), we can write

$$\hat{G}(x, t; x_0, t_0) = \theta(t - t_0) \sum_n e^{-iE_n(t-t_0)} u_n(x) u_n^*(x_0) \quad (8)$$

or equivalently its Fourier transform

$$\tilde{G}(t, t_0; z) = i \sum_n \frac{1}{z - E_n} u_n(x) u_n^*(x_0) \quad (9)$$

From (9) it is clear why \hat{G} contains all the information about the dynamics: \hat{H} has real eigenvalues and so \hat{G} has singularities along the real axis. Bounded states are poles for $Re(z) < 0$ and $Im(z) = 0$.

II. INTERPRETATION AND PROPERTIES OF \hat{G}

$\hat{G}(x_N, T; x_0, t_0)$ has the following physical interpretation: it is the probability amplitude that a system is measured at position x_N at time t_N , if it was at x_0 at time t_0 .

The important property, which is at the basis of the Feynman path integral formulation, is the convolution property

$$\hat{G}(x_N, T; x_0, t_0) = \int dx_1 [\hat{G}(x_N, T; x_1, t_1) \hat{G}(x_1, t_1; x_0, t_0)]$$

It states that the probability amplitude is the sum of all possible products of probability amplitudes, where, for possible, one intends over all the possible positions x_1 . If we iterate this procedure N times, then we are summing over all the possible paths (see figure (1)).

$$\hat{G}(x_N, T; x_0, t_0) = \int dx_1 \dots dx_N [\hat{G}(x_N, T; x_1, t_1) \dots \hat{G}(x_{i-1}, t_{i-1}; x_i, t_i) \dots \hat{G}(x_{N-1}, t_{N-1}; x_0, t_0)]$$

The time is made discrete on a lattice with lattice spacing $a = T/N$, where $T = (t - t_0)$. Then we can write the evolution as the product of evolutions over each time slice. As a consequence the retarded propagator can be written as ¹

$$\begin{aligned} \hat{G}(t, t_0) &= e^{-iaN\hat{H}} = e^{-iaN\left(\frac{\hat{p}^2}{2m} + V(\hat{x})\right)} \\ &\simeq \left[e^{-ia\frac{\hat{p}^2}{2m}} e^{-iaV(\hat{x})} \right]^N = \\ &= e^{-\frac{iaV(\hat{x})}{2}} \left[e^{-\frac{iaV(\hat{x})}{2}} e^{-ia\frac{\hat{p}^2}{2m}} e^{-\frac{iaV(\hat{x})}{2}} \right]^N e^{-\frac{iaV(\hat{x})}{2}} \end{aligned} \quad (10)$$

¹Here we make use of the **Trotter formula**, which states that given two reasonable operators A and B (where reasonable means that their commutator $[A, B]$ does not explode), the following limit holds

$$e^{(A+B)} = \lim_{N \rightarrow +\infty} \left(e^{\frac{A}{N}} e^{\frac{B}{N}} \right)^N$$

Proof. From exponential expansion we can write

$$e^{\frac{A+B}{N}} = e^{\frac{A}{N}} e^{\frac{B}{N}} + o\left(\frac{1}{N^2}\right)$$

Now we evaluate the difference

$$\begin{aligned} \left(e^{\frac{A}{N}} e^{\frac{B}{N}} \right)^N - \left(e^{\frac{A+B}{N}} \right)^N &= - \left(e^{\frac{A+B}{N}} \right) \left(e^{\frac{A+B}{N}} \right)^{N-1} + e^{\frac{A}{N}} e^{\frac{B}{N}} e^{\frac{A+B}{N}(N-1)} - e^{\frac{A}{N}} e^{\frac{B}{N}} e^{\frac{A+B}{N}(N-1)} + \dots - \left(e^{\frac{A}{N}} e^{\frac{B}{N}} \right)^{N-1} e^{\frac{A+B}{N}} + \left(e^{\frac{A}{N}} e^{\frac{B}{N}} \right)^N = \\ &= \left[-e^{\frac{A+B}{N}} + e^{\frac{A}{N}} e^{\frac{B}{N}} \right] e^{\frac{A+B}{N}(N-1)} + e^{\frac{A}{N}} e^{\frac{B}{N}} \left[-e^{\frac{A+B}{N}} + e^{\frac{A}{N}} e^{\frac{B}{N}} \right] e^{\frac{A+B}{N}(N-2)} + \dots + e^{\frac{A}{N}} e^{\frac{B}{N}} \left[-e^{\frac{A+B}{N}} + e^{\frac{A}{N}} e^{\frac{B}{N}} \right] = \\ &= 0 + o\left(\frac{1}{N^2}\right) \end{aligned}$$

□

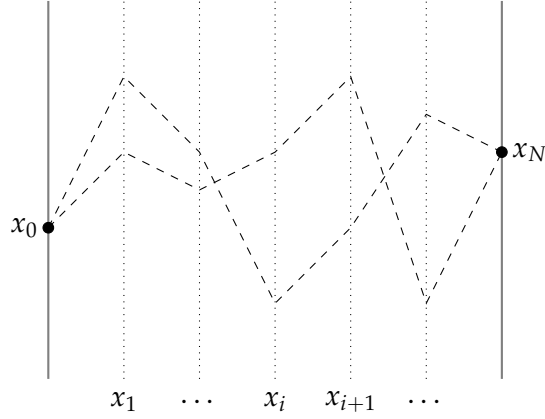


Figure 1: Illustration of two possible paths between two fixed endpoints, x_0 and x_N

ii.1 Transfer operator

We define the transfer operator $\hat{\mathcal{T}}_a$, the one that evolves the system over a time interval $\delta t = a$, as

$$\hat{\mathcal{T}}_a = e^{-\frac{iaV(\hat{x})}{2}} e^{-ia\frac{\hat{p}^2}{2m}} e^{-\frac{iaV(\hat{x})}{2}} \quad (11)$$

Therefore

$$\hat{G}(t, t_0) = e^{\frac{iaV(\hat{x})}{2}} [\hat{\mathcal{T}}_a]^N e^{-\frac{iaV(\hat{x})}{2}} \quad (12)$$

Since the transfer operator is, by definition, a unitary operator

$$\hat{\mathcal{T}}_a \hat{\mathcal{T}}_a^\dagger = \hat{\mathcal{T}}_a^\dagger \hat{\mathcal{T}}_a = \mathbb{1}$$

we can define an operator \hat{H} such that

$$\hat{\mathcal{T}}_a = e^{-ia\hat{H}}, \quad \hat{H} = \hat{H}^\dagger \quad (13)$$

In the continuum limit $a \rightarrow 0$, we have that $\hat{H} \rightarrow \hat{H}$. If we name with $|\epsilon_n\rangle$ the transfer operator eigenstates, then

$$\hat{\mathcal{T}}_a |\epsilon_n\rangle = e^{-ia\epsilon_n} |\epsilon_n\rangle \quad (14)$$

then the following relation holds

$$\epsilon_n = E_n + o(a^2) \quad (15)$$

where the difference between the retarded propagator eigenvalues and the transfer operator ones lies in discretization errors only.

ii.2 Analytic continuation to the Euclidean propagator

We now perform the Wick rotation to pass from the Minkowski retarded propagator to the Euclidean one, so that the integrals involved are well defined and convergent.

$$\hat{G}_E(t, t_0) = \hat{G}(-it, -it_0), \quad \text{where } t_E = it \quad (16)$$

t_E is the Euclidean time, it is a real variable and it corresponds to the imaginary part of t analytically continued. The Euclidean propagator contains all the information on the dynamics of the system as well.

The time interval is as before $[0, T]$, with $t_E = an$, $n = 0, 1, \dots, N$. Therefore under $a \rightarrow -ia_E$, the Euclidean transfer operator becomes

$$\hat{T}_{a_E} = e^{-\frac{a_E}{2}V(\hat{x})} e^{-\frac{p^2}{2m}a_E} e^{-\frac{a_E}{2}V(\hat{x})} \quad (17)$$

The preceding relations (13), (14) and (15) are modified as follows²

$$\hat{T}_a = e^{-a\hat{H}} = e^{-a\hat{H}} + o(a^2) \quad (18)$$

$$\hat{T}_a|\epsilon_n\rangle = e^{-a\epsilon_n}|\epsilon_n\rangle \quad (19)$$

$$\epsilon_n = E_n + o(a^2) \quad (20)$$

Since

$$\hat{T}_a^N = \hat{T}_a \int dx_1 |x_1\rangle \langle x_1| \hat{T}_a \int dx_2 |x_2\rangle \langle x_2| \hat{T}_a \dots$$

for each time interval a we are going to evaluate

$$\langle x_i | \hat{T}_a | x_{i+1} \rangle = \langle x_i | e^{-\frac{a}{2}V(\hat{x})} e^{-\frac{p^2}{2m}a} e^{-\frac{a}{2}V(\hat{x})} | x_{i+1} \rangle$$

By definition we have that

$$e^{-\frac{a}{2}V(\hat{x})} | x_i \rangle = e^{-\frac{a}{2}V(x_i)} | x_i \rangle \quad (21)$$

On the other hand the kinetic term can be written as

$$\begin{aligned} \langle x_i | e^{-\frac{p^2}{2m}a} | x_{i+1} \rangle &= \int dp \langle x_i | p \rangle \langle p | e^{-\frac{p^2}{2m}a} | x_{i+1} \rangle \\ &= \int dp \langle x_i | p \rangle e^{-\frac{p^2}{2m}a} \langle p | x_{i+1} \rangle \\ &= \frac{1}{2\pi} \int dp e^{ipx_i} e^{-\frac{p^2}{2m}a} e^{-ipx_{i+1}} \\ &= \left(\frac{m}{2\pi a} \right)^{1/2} e^{-\frac{(x_i - x_{i+1})^2 m}{2a}} \end{aligned} \quad (22)$$

²From now on the subscript E could be dropped, it will be clear from the context whether we are working in the Euclidean or in the Minkowski time

where we have used the normalization property $\langle x|p\rangle = \frac{1}{\sqrt{2\pi}}e^{ipx}$ and performed a gaussian integration³. Putting together the two pieces in (21) and (22), we obtain that

$$\langle x_i|\hat{T}_a|x_{i+1}\rangle = \left(\frac{m}{2\pi a}\right)^{1/2} e^{-a\left[\frac{m}{2}\left(\frac{x_i-x_{i+1}}{a}\right)^2 + \frac{1}{2}V(x_i) + \frac{1}{2}V(x_{i+1})\right]} \quad (23)$$

We now can turn back to our Euclidean propagator and write it as a path integral in the following way

$$\begin{aligned} \langle x_N|\hat{G}(T)|x_0\rangle &\simeq e^{\frac{aV(x_N)}{2}} \langle x_N|\hat{T}_a \int dx_{N-1}|x_{N-1}\rangle \langle x_{N-1}|\hat{T}_a \int dx_{N-2} \dots \hat{T}_a|x_0\rangle e^{-\frac{aV(x_0)}{2}} \\ &= \int \prod_{i=1}^{N-1} dx_i e^{\frac{a}{2}V(x_N)} \left[\prod_{j=0}^{N-1} \langle x_{j+1}|\hat{T}_a|x_j\rangle \right] e^{-\frac{a}{2}V(x_0)} \\ &= \left(\frac{m}{2\pi a}\right)^{N/2} \int \prod_{i=0}^{N-1} dx_i \prod_{j=0}^{N-1} e^{-a\left[\frac{m}{2}\left(\frac{x_{j+1}-x_j}{a}\right)^2 + V(x_j)\right]} \end{aligned}$$

If we define the Euclidean Lagrangian density as

$$\mathcal{L}_E(x_{i+1}, x_i) \equiv \frac{m}{2} \left(\frac{x_{i+1} - x_i}{a}\right)^2 + V(x_i) \quad (24)$$

and call Euclidean action

$$\mathcal{S}_E = a \sum_{i=0}^{N-1} \mathcal{L}_E(x_{i+1}, x_i) \quad (25)$$

then

$$G_E(x_N, T, x_0, 0) = \left(\frac{m}{2\pi a}\right)^{N/2} \int \prod_{i=1}^{N-1} dx_i e^{-\mathcal{S}_E}, \quad \text{with fixed } x_0, x_N \quad (26)$$

This is the retarded propagator expressed as a path integral of a quantistic system in the Euclidean.

ii.3 Back to Minkowski

To come back to Minkowski we perform

$$a_E \rightarrow ia$$

and obtain

$$\mathcal{L} = -\mathcal{L}_E(x_{i+1}, x_i)|_{a_E \rightarrow ia} = \frac{m}{2} \left(\frac{x_{i+1} - x_i}{a}\right)^2 - V(x_i)$$

³The formula for a Gaussian integral is given by

$$\frac{1}{\sqrt{2\pi\sigma^2}} \int_{-\infty}^{+\infty} dq e^{-\frac{q^2}{2\sigma^2}} e^{iqx} = e^{-\frac{x^2\sigma^2}{2}}$$

$$\mathcal{S} = a \sum_{i=0}^{N-1} \mathcal{L}(x_{i+1}, x_i)$$

$$G(x_N, T; x_0, 0) = \left(\frac{m}{2\pi i a} \right)^{N/2} \int \prod_{i=1}^{N-1} dx_i e^{i\mathcal{S}}$$

Thus written, this integral makes sense only as a concise way to indicate the procedure above illustrated; in other words as an analytic continuation of the retarded propagator in the Euclidean. In fact, we have to consider $a \neq 0$, analytically continue G using the path integral formalism, then come back to Minkowski and take the limit $a \rightarrow 0$.

ii.4 Physical meaning of the path integral formalism

The path integral formalism is a powerful tool that takes into account quantum effects. In classical mechanics a particle moves along a trajectory $x(t)$, given extremizing its action. The equations of motion are the Lagrange equations

$$\frac{d}{dt} \left(\frac{\partial \mathcal{L}}{\partial \dot{x}} \right) - \frac{\partial \mathcal{L}}{\partial x} = 0$$

and this implies that, in classical mechanics, the motion of the particle is determined only by the form of the action S around its extremum.

In quantum mechanics, instead, all the possible trajectories contribute with a probability amplitude given by

$$\int \prod_i dx_i e^{i\frac{\mathcal{S}}{\hbar}}$$

and, as a consequence, not only the form of S is relevant but also its value, since it defines the weight of the trajectories.

In particular, for a classical system $|\mathcal{S}| \gg \hbar$, and, in general, trajectories have different phases and cancel each other: trajectories far from the minimum of the action do not contribute, only those with $\delta\mathcal{S} \sim \hbar$ contribute, where with $\delta\mathcal{S}$ we intend the difference in action between a generic trajectory and the stationary one.

For a quantum system, instead, $\delta\mathcal{S} \sim \hbar$ for all the trajectories and so all the paths contribute.

III. CONNECTION WITH STATISTICAL MECHANICS: PARTITION FUNCTION AND NUMERICAL METHODS

Here we illustrate the advantages of the path integral formalism along with numerical tools.

We can define the partition function as

$$Z_a = \left(\frac{m}{2\pi a} \right)^{N/2} \int \prod_{i=0}^{N-1} dx_i e^{-\mathcal{S}_E}$$

and we can see that it is analogous to the partition function in statistical mechanics, with the Boltzmann factor replacing e^{-S_E} .

When periodic boundary conditions are imposed, then Z_a can be easily written in operatorial form as follows

$$Z_a = \left(\frac{m}{2\pi a}\right)^{N/2} \int \prod_{i=0}^{N-1} dx_i e^{-S_E} = \text{Tr} [\hat{G}_E(T, t_0)] = \text{Tr} [\hat{T}_a^N] \quad (27)$$

Quite always the normalization factor $\left(\frac{m}{2\pi a}\right)^{N/2}$ is negligible.

It follows that

$$Z_a = \sum_n e^{-aN\epsilon_n}$$

and therefore, from Z_a , it is possible to extract the energy eigenvalues.

In general, in quantum mechanics, we are interested in calculating matrix elements of operators, for example those between eigenstates of the hamiltonian \hat{H} . It is possible to extract the matrix elements using the path integral formalism. We start from the definition of the two-point correlation function

$$C(t_k, t_j) = \frac{\int \prod_{i=0}^{N-1} dx_i [e^{-S} \hat{O}_1(x_k) \hat{O}_2(x_j)]}{\int \prod_{i=0}^{N-1} dx_i [e^{-S}]} = \frac{\int \prod_{i=0}^{N-1} dx_i [e^{-S} \hat{O}_1(x_k) \hat{O}_2(x_j)]}{Z_a} \quad (28)$$

Monte Carlo methods enter here as we extract trajectories with probability distribution given by e^{-S} .

We can show that under suitable limits⁴, (28) is equal to the T-product of operators

$$\lim_{T \rightarrow +\infty} C(t_k, t_j) = \langle \epsilon_0 | \hat{T}(\hat{O}_1 \hat{O}_2) | \epsilon_0 \rangle$$

and

$$\lim_{a \rightarrow 0} \langle \epsilon_0 | \hat{T}(\hat{O}_1 \hat{O}_2) | \epsilon_0 \rangle = \langle E_0 | \hat{T}(\hat{O}_1 \hat{O}_2) | E_0 \rangle$$

⁴ Here we give a concise demonstration of the double limit

Proof. Given

$$Z_a(T) = \text{Tr} [\hat{T}_a^N] = \sum_n e^{-aN\epsilon_n} = \sum_n e^{-T\epsilon_n}, \quad aN = T$$

then using the identity $\hat{\mathcal{I}} = \sum_n |\epsilon_n\rangle \langle \epsilon_n|$

$$C(t_k, t_j) \cdot Z_a(T) = \theta(t_j - t_k) \sum_n e^{-\epsilon_n(T-|t_k-t_j|)} \langle \epsilon_n | \hat{O}_2 \hat{T}^{|t_k-t_j|} \hat{O}_1 | \epsilon_n \rangle + \theta(t_k - t_j) \sum_n e^{-\epsilon_n(T-|t_k-t_j|)} \langle \epsilon_n | \hat{O}_1 \hat{T}^{|t_k-t_j|} \hat{O}_2 | \epsilon_n \rangle$$

In the limit $\lim_{T \rightarrow +\infty}$ only the vacuum contribution ϵ_0 survives. Therefore

$$\begin{aligned} \lim_{a \rightarrow 0} \lim_{\substack{T \rightarrow +\infty \\ (a=\text{const})}} C(t_k, t_j) &= \theta(t_j - t_k) \langle E_0 | \hat{O}_2(t_j) \hat{O}_1(t_k) | E_0 \rangle + \theta(t_k - t_j) \langle E_0 | \hat{O}_1(t_k) \hat{O}_2(t_j) | E_0 \rangle \\ &= \langle E_0 | \hat{T}(\hat{O}_1(t_k) \hat{O}_2(t_j)) | E_0 \rangle \end{aligned}$$

□

It is this double limit that shows how the path integral can be useful.

Along with the correlation functions path integrals are used to calculate expectations values of observables

$$\langle \hat{O} \rangle = \frac{1}{Z} \int [\mathcal{D}x] e^{-S} \hat{O}(x) \tag{29}$$

where we indicate with $[\mathcal{D}x]$ the integration over all the trajectories. As before, Monte Carlo methods are used to extract paths with probability $\frac{1}{Z}e^{-S}$.

In both (28) and (29), the Central Limit Theorem assures that the best estimate of an integral

$$I = \int dx [f(x)P(x)]$$

is given by

$$\bar{I} = \frac{1}{N_{\text{conf}}} \sum_{i=0}^{N_{\text{conf}}-1} f(x_i)$$

where x_i are the paths generated with Monte Carlo methods according to the distribution probability $P(x)$ (in our case it is $\frac{1}{Z}e^{-S}$) and N_{conf} is the number of the extracted trajectories. This automatically generalizes to d dimensions.

IV. OUTLINE OF THE PROJECT

In this work two quantum systems are taken into consideration: the harmonic oscillator and a scalar field theory. Both require Monte Carlo methods to numerically evaluate the integrals involved in the theory. We implement Markov Chain Monte Carlo methods to generate large samples of system configurations, distributed according to $\frac{1}{Z}e^{-S}$.

In the next section (II) MCMC methods are analyzed in detail. Then the Metropolis algorithm is implemented in the case of the harmonic oscillator in section (III), whereas the Hamiltonian Monte Carlo (HMC) is implemented to simulate the scalar theory in section (IV).

In the appendix, the statistical error analysis using jackknife method is discussed and a scheme⁵ for both programs is provided.

⁵The project is divided into two parts: LFC18 implements the harmonic oscillator, whereas phi4 implements the $\lambda\phi^4$ theory.

II. NUMERICAL METHODS: MCMC

I. MARKOV CHAIN MONTE CARLO (MCMC)

To analyze the two quantum systems, the harmonic oscillator and the scalar field, we have to implement numerical methods in order to evaluate the correlation functions and the expectation values of observables. Such methods are part of the Monte Carlo methods.

The term Monte Carlo is used for calculational techniques which make use of random numbers to construct samples distributed according to some fixed probability density. In our work we implement a Markov Chain Monte Carlo (MCMC) algorithm.

The idea behind MCMC methods is to generate samples from a target distribution π by the means of a Markov chain whose stationary probability density is indeed π . A Markov chain is a sequence of random variables $(x_0, x_1, x_2, \dots, x_n)$ such that x_i depends only on x_{i-1} .

Formally a sequence of events is a Markov chain if

$$P(x_{j_0}, \dots, x_{j_n}) = a_{j_0} P_{j_0 j_1} \dots P_{j_{n-1} j_n}$$

where a_{j_0} is an arbitrary first element of the chain, with

$$a_{j_0} \geq 0, \quad \sum_{j_0} a_{j_0} = 1$$

and

$$P_{j_0 j_1} \geq 0, \quad \sum_{j_1} P_{j_0 j_1} = 1$$

To each Markov chain is associated a transition matrix, given by

$$P = \begin{bmatrix} P_{11} & P_{12} & P_{13} & \dots \\ P_{21} & P_{22} & P_{23} & \dots \\ P_{31} & P_{32} & P_{33} & \dots \\ \dots & \dots & \dots & \dots \end{bmatrix}$$

This type of matrices satisfy

$$P_{ij} \geq 0, \quad \forall i, j, \quad \sum_j P_{ij} = 1$$

and are called stochastic matrices.

II. ERGODIC THEOREM AND ASYMPTOTIC DISTRIBUTION

An interesting point is to study under what conditions a Markov chain converges to a stationary distribution, so to assure that the trajectories follow the desired probability density, after the procedure is repeated a large number of times. Here comes the ergodic theorem.

If we perform n steps, with $\lim_{n \rightarrow +\infty}$, then the ergodic theorem⁶ assures that, if we are dealing with an ergodic Markov chain, then

$$\lim_{n \rightarrow +\infty} [P]_{ij}^{(n)} = \pi_j$$

A Markov chain is said to be ergodic when each state x_j in the configuration space is persistent (the probability to extract it again after the first extraction is 1), not null (its mean recurrence time is $\mu_j < +\infty$) and aperiodic.

If the Markov chain is ergodic, it will converge to its stationary distribution independently of its initial conditions, thanks to the ergodic theorem.

A sufficient but not necessary condition to guarantee ergodicity is to demand that the detailed balance condition

$$\pi_i P_{ij} = \pi_j P_{ji} \tag{30}$$

is satisfied. This condition requires that the probabilities of moving from state x_i to x_j and from x_j to x_i are the same.

In our case the desired asymptotic distribution is $\pi = \frac{1}{Z} e^{-\mathcal{S}}$. The only problem is to find a stochastic matrix P that satisfies (30). In the following section we will analyze two methods to generate ergodic Markov chains: the Metropolis algorithm and the Hamiltonian Monte Carlo one.

⁶The ergodic theorem states that

Theorem 1 (Ergodic theorem). *x_i are ergodic states and there exists the limit*

$$\lim_{n \rightarrow +\infty} [P_{jk}]^{(n)} = \pi_k$$

if and only if

$$\sum_k \pi_k = 1, \quad \pi_k = \sum_i \pi_i P_{ik}$$

III. METROPOLIS MONTE CARLO: HARMONIC OSCILLATOR

I. HARMONIC OSCILLATOR IN 1-D

The harmonic oscillator is one of the few systems that can be solved analytically and here will serve us as a test case for Monte Carlo methods. We perform our simulation in the Euclidean time. The hamiltonian of the system is given by

$$\hat{H} = \frac{\hat{p}^2}{2m} + \frac{1}{2}m\omega^2\hat{x}^2 \quad (31)$$

and the discretized action is

$$\mathcal{S}(x_i) = a \sum_{i=0}^{N-1} \left\{ \frac{m}{2} \left(\frac{x_{i+1} - x_i}{a} \right)^2 + \frac{1}{2}m\omega^2 x_i^2 \right\} \quad (32)$$

The partition function is given by

$$Z = \int \prod_{i=0}^{N-1} dx_i e^{-\mathcal{S}(x_i)} \quad (33)$$

Periodic boundary conditions have been used: $x(0) = x(Na)$, where we use x to label the position, a to denote the time lattice spacing ($\delta t = a$) and N represents the number of points on our time lattice. In our simulation $m = \omega = 1$. Where not otherwise specified, $a = 1$ and $N = 64$. All these parameters are defined in the *global.h* file.

The main objective of this simulation is to calculate the two-point correlation function for the position operator, which according to (28) is

$$C(t) = \langle \hat{x}_i \hat{x}_{i+t} \rangle = \frac{1}{Z} \int \prod_{i=0}^{N-1} dx_i e^{-\mathcal{S}} \hat{x}_i \hat{x}_{i+t} \quad (34)$$

where t is the physical time over which the system evolves.

We can rewrite (34) using operator tools and obtain

$$\langle \hat{x}_i \hat{x}_{i+t} \rangle = \frac{1}{\text{Tr}[\hat{T}^N]} \text{Tr} \left[\hat{T}^{N-t} \hat{x} \hat{T}_a^t \hat{x} \right] \quad (35)$$

where \hat{T} is the evolution operator defined in (17).

From (35) we can extract both the energy difference between the fundamental and the first excited state, $\Delta\epsilon = \epsilon_1 - \epsilon_0$, and the matrix element $|\langle \epsilon_0 | \hat{x} | \epsilon_1 \rangle|^2$, where with $|\epsilon_i\rangle$ we denote the transfer operator eigenstates as in (19).

We analyze separately the numerator and the denominator of (35)

$$\text{Tr}[\hat{T}^N] = \sum_j e^{-aN\epsilon_j} \xrightarrow{N \rightarrow \infty} e^{-aN\epsilon_0}$$

since for large N all the contributions are suppressed except for the vacuum one. For the denominator we use the identity $\mathbb{1} = \sum_j |\epsilon_j\rangle\langle\epsilon_j|$

$$\text{Tr}[\hat{T}^{N-t}\hat{x}\hat{T}^t\hat{x}] = \sum_{i,j} e^{-a(N-t)\epsilon_i} e^{-ate_j} \langle\epsilon_i|\hat{x}|\epsilon_j\rangle\langle\epsilon_j|\hat{x}|\epsilon_i\rangle$$

taking the limit for $N \rightarrow +\infty$ only the vacuum and the first excited states survive

$$\xrightarrow{N \rightarrow \infty} \sum_j e^{-a(N-t)\epsilon_0} e^{-ate_j} \langle\epsilon_0|\hat{x}|\epsilon_j\rangle\langle\epsilon_j|\hat{x}|\epsilon_0\rangle + e^{-a(N-t)\epsilon_1} e^{-ate_0} \langle\epsilon_1|\hat{x}|\epsilon_0\rangle\langle\epsilon_0|\hat{x}|\epsilon_1\rangle \quad (36)$$

Putting together the two pieces, we obtain

$$C(t) \xrightarrow{N \rightarrow \infty} \left\{ |\langle\epsilon_0|\hat{x}|\epsilon_1\rangle|^2 e^{-\frac{N}{2}a(\epsilon_1-\epsilon_0)} \cdot 2 \cosh\left[\left(\frac{N}{2} - t\right)a(\epsilon_1 - \epsilon_0)\right] \right\} \cdot \frac{1}{e^{-aN\epsilon_0}} \quad (37)$$

We call R

$$R = 2 |\langle\epsilon_0|\hat{x}|\epsilon_1\rangle|^2 e^{-\frac{N}{2}a(\epsilon_1-\epsilon_0)}$$

we have that

$$C(t) \xrightarrow[N \rightarrow \infty]{t \gg 1} R \cosh\left(\left(\frac{N}{2} - t\right)a\Delta\epsilon\right)$$

The value of $\Delta\epsilon$ can be extracted from the correlator as follows⁷

$$\Delta\epsilon(t) = \frac{1}{a} \cosh^{-1} \left[\frac{C(t+1) + C(t-1)}{2C(t)} \right] \quad (38)$$

Then the matrix element can be calculated

$$|\langle\epsilon_0|\hat{x}|\epsilon_1\rangle|(t) = \sqrt{\frac{C(t)e^{\frac{N}{2}a\Delta\epsilon}}{2 \cosh\left[\left(\frac{N}{2} - t\right)a\Delta\epsilon(t)\right]}} \quad (39)$$

In this first part we want to calculate (38) and (39) so that we can confront the results with the theoretical expected values. Our primary variable is the correlator (34) and we have to implement a MCMC method to generate paths according to the distribution given by the path integral $\frac{1}{Z}e^{-\mathcal{S}}$, which plays the role of the desired asymptotic distribution. In order for the trajectories to converge to this probability, we guarantee that the detailed balance is satisfied using a Metropolis algorithm.

⁷It is sufficient to write explicitly the three terms using (36)

$$\begin{aligned} C(t) &= \text{const} \left[e^{-aN\epsilon_0} e^{-at(\epsilon_1-\epsilon_0)} + e^{-aN\epsilon_1} e^{-at(\epsilon_0-\epsilon_1)} \right] \\ C(t+1) &= \text{const} \left[e^{-aN\epsilon_0} e^{-at(\epsilon_1-\epsilon_0)} e^{-a(\epsilon_1-\epsilon_0)} + e^{-aN\epsilon_1} e^{-at(\epsilon_0-\epsilon_1)} e^{-a(\epsilon_0-\epsilon_1)} \right] \\ C(t-1) &= \text{const} \left[e^{-aN\epsilon_0} e^{-at(\epsilon_1-\epsilon_0)} e^{a(\epsilon_1-\epsilon_0)} + e^{-aN\epsilon_1} e^{-at(\epsilon_0-\epsilon_1)} e^{a(\epsilon_0-\epsilon_1)} \right] \end{aligned}$$

Then it simply follows that

$$C(t+1) + C(t-1) = 2 \cosh(a\Delta\epsilon(t))C(t)$$

II. METROPOLIS ALGORITHM

The most important attribute of this algorithm is the use of importance sampling, in other words random points are generated with higher probability in the region of interest.

Given the action of the system \mathcal{S} , as in (32), each Markov chain is a sequence of position values $(x_0, x_1, \dots, x_i, \dots, x_{N-1})$, where N is defined as before. The following scheme explains the mechanism:

1. Generate any random initial path $(x_0, x_1, \dots, x_i, \dots, x_{N-1})$
2. Choose the random point x'_i with uniform probability within the interval

$$x_i - \Delta < x'_i < x_i + \Delta$$

where $\Delta = 1$

3. Replace x_i with the new value x'_i and calculate the difference in action

$$\Delta\mathcal{S}(x'_i, x_i) \equiv \mathcal{S}(x'_i) - \mathcal{S}(x_i)$$

4. If $\Delta\mathcal{S}(x'_i, x_i) < 0$, i.e. the action is lowered by replacing the value at i with x'_i , then the replacement occurs
5. If $\Delta\mathcal{S}(x'_i, x_i) \geq 0$, then generate a random number $r \in [0, 1]$
 - if $e^{-\Delta\mathcal{S}(x'_i, x_i)} > r$, then accept the new point x'_i , change the initial path and pass to the next point
 - otherwise reject x'_i (keep x_i) and pass to the next point

With this choice of the transition probability, the detailed balance condition is satisfied and so we assure that, after many iterations (we generate $N_{\text{conf}} = 10^6$ paths), the paths are generated following the required distribution.

ii.1 Thermalization: reaching equilibrium

We start our simulation with a random path $x_{i+1} = (-1)x_i$, $x_0 = -1$. We can see by looking at the value of the action (see figure (2)) that, at the beginning, the new paths are not in equilibrium. After few iterations the value of the action settles down and there are just statistical fluctuations. We say that we are in thermal equilibrium. By taking measurements over many such paths, values of observables may then be calculated. The primary observable involved in our calculations is the correlator as defined in (34).

ii.2 Correlation function

Once the paths are generated according to the equilibrium distribution, the correlation function can be calculating using the results of the Central Limit Theorem

$$C^\xi(t) = \frac{1}{N} \sum_{i=0}^{N-1} x_i^\xi x_{i+t}^\xi \quad (40)$$

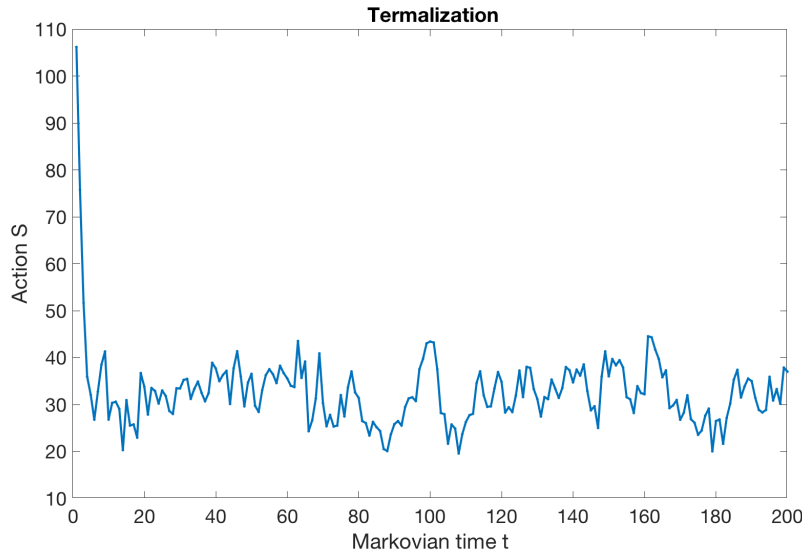


Figure 2: The action values are plotted as functions of the markovian time. We can see how after few iterations it thermalizes.

where ζ is the configuration index. If we want to take the mean over the N_{conf} values, we have to pay attention to the fact that, by definition of the Markov chain, two successive paths are correlated.

ii.3 Autocorrelation function: how to uncorrelate data

Since the values evaluated using (40) are correlated, the statistic uncertainty of the value of the correlator, at a fixed physical time, averaged over N_{conf} , $\bar{C}(t)$, would be complicated to calculate.

Starting from

$$\sigma_{\bar{C}}^2 = \langle \bar{C}^2 \rangle - \langle \bar{C} \rangle^2$$

we can expand

$$\begin{aligned} \langle \bar{C}^2 \rangle &= \frac{1}{N_{\text{conf}}} \sum_{\zeta_i, \zeta_j} \langle C_{\zeta_i} C_{\zeta_j} \rangle \\ &= \frac{1}{N_{\text{conf}}} \sum_{\zeta_i} \langle C_{\zeta_i}^2 \rangle + \frac{2}{N_{\text{conf}}} \sum_{\zeta_i \neq \zeta_j} \langle C_{\zeta_i} C_{\zeta_j} \rangle \end{aligned}$$

Then

$$\sigma_{\bar{C}}^2 = \frac{1}{N_{\text{conf}}} \sum_{\zeta_i} [\langle C_{\zeta_i}^2 \rangle - \langle C_{\zeta_i} \rangle^2] + \frac{2}{N_{\text{conf}}} \sum_{\zeta_i \neq \zeta_j} [\langle C_{\zeta_i} C_{\zeta_j} \rangle - \langle C \rangle^2]$$

If the data were not correlated we would simply have

$$\langle C_{\zeta_i} C_{\zeta_j} \rangle = \langle C_{\zeta_i} \rangle \langle C_{\zeta_j} \rangle = \langle C \rangle^2 \quad \implies \quad \sigma_{\bar{C}}^2 = \frac{1}{N_{\text{conf}}} [\langle C^2 \rangle - \langle C \rangle^2]$$

But if they are correlated

$$\begin{aligned}\sigma_C^2 &= \frac{1}{N_{\text{conf}}} [\langle C^2 \rangle - \langle C \rangle^2] \left[1 + 2 \sum_{\xi_i \neq \xi_j} \frac{\langle C_{\xi_i} C_{\xi_j} \rangle - \langle C \rangle^2}{\langle C^2 \rangle - \langle C \rangle^2} \right] = \\ &= \frac{1}{N_{\text{conf}}} [\langle C^2 \rangle - \langle C \rangle^2] \left[1 + 2 \sum_{\xi_i=1}^{N_{\text{conf}}} \sum_{\xi_j=1}^{N_{\text{conf}}-1} \frac{\langle C_{\xi_i} C_{\xi_i+\xi_j} \rangle - \langle C \rangle^2}{\langle C^2 \rangle - \langle C \rangle^2} \right]\end{aligned}$$

Considering an infinite number of configurations, we can write

$$\sigma_C^2 = \frac{1}{N_{\text{conf}}} [\langle C^2 \rangle - \langle C \rangle^2] \left[1 + 2 \sum_{\xi_i=1}^{N_{\text{conf}}} \sum_{\xi_j=1}^{N_{\text{conf}}} \frac{\langle C_{\xi_i} C_{\xi_i+\xi_j} \rangle - \langle C \rangle^2}{\langle C^2 \rangle - \langle C \rangle^2} \right]$$

Then we define the autocorrelation function as

$$\Gamma(t) = \frac{\langle C_{\xi_i} C_{\xi_i+\xi_j} \rangle - \langle C \rangle^2}{\langle C^2 \rangle - \langle C \rangle^2} \quad (41)$$

The autocorrelation function can be used to obtain a sample of uncorrelated data.

The plot in figure (3) shows the autocorrelation function of our correlator data. It allows to estimate how many iteration are required in order for them to be uncorrelated.

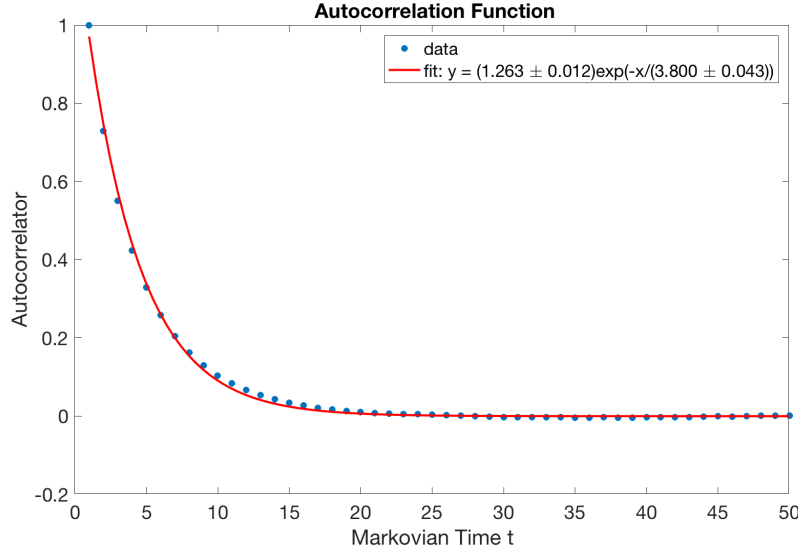


Figure 3: The autocorrelation function Γ is fitted with an exponential of the type $ae^{(-t/\tau)}$, where $\tau \sim 3.8$ is linked to the correlation time (the time we are referring to is the Markovian time)

The autocorrelation function decays exponentially following

$$\Gamma(t) \sim e^{-t/\tau}$$

where τ is the autocorrelation time. The fitting function that overlaps the data has $\tau \sim 3.8$. This value is needed to determine the dimension of the bin. In fact, two paths stay correlated as long as there are enough iterations in between them. Taking the average of the correlator every 10τ (or more) configurations, the new data, now uncorrelated, can be used for calculating the observables. This procedure, called binning, produces $N_{\text{conf}}/D_{\text{bin}}$ number of independent measures, where D_{bin} is the dimension of the bin (in our case we took $D_{\text{bin}} = 50$). Thus the standard deviation estimate can easily be done as explained in the appendix (IV).

Returning to the correlation function, we can see in figure (4) a logarithmic plot of correlator, averaged on the N_{conf} sample, for different values of N_{conf} . We see how its values oscillate around the zero point.

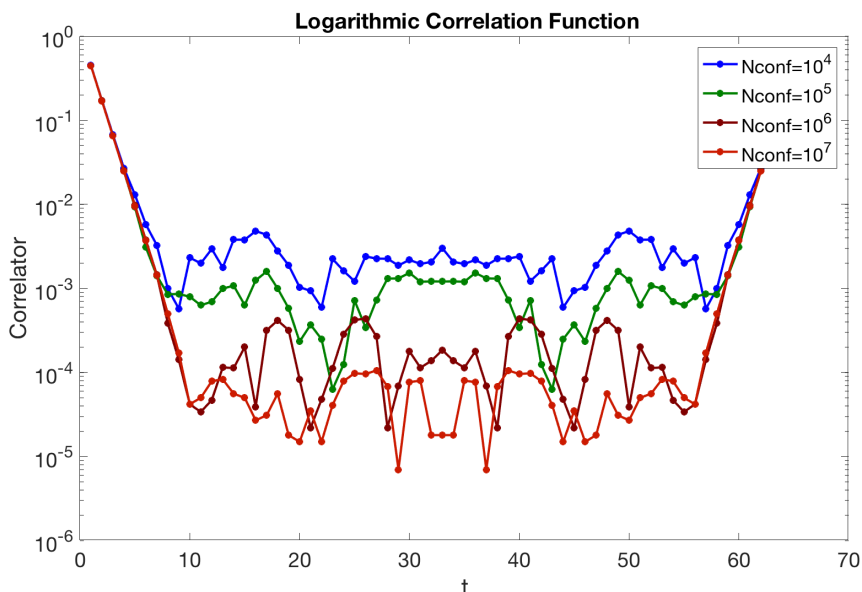


Figure 4: Correlation function plotted in logarithmic scale for different values of N_{conf}

An interesting feature can be noticed if we plot the correlator for a fixed N_{conf} with its error line, as we can see in the plots of figure (5). In fact, in each case, the error value is of the same order of the correlator value. This means that the ratio

$$\frac{\sigma_{\bar{C}}}{\bar{C}(t)} \sim \frac{1}{\sqrt{N_{\text{conf}}}} \rightarrow 1$$

The oscillations of the correlator are of the same size of the error and the results are no longer reliable.

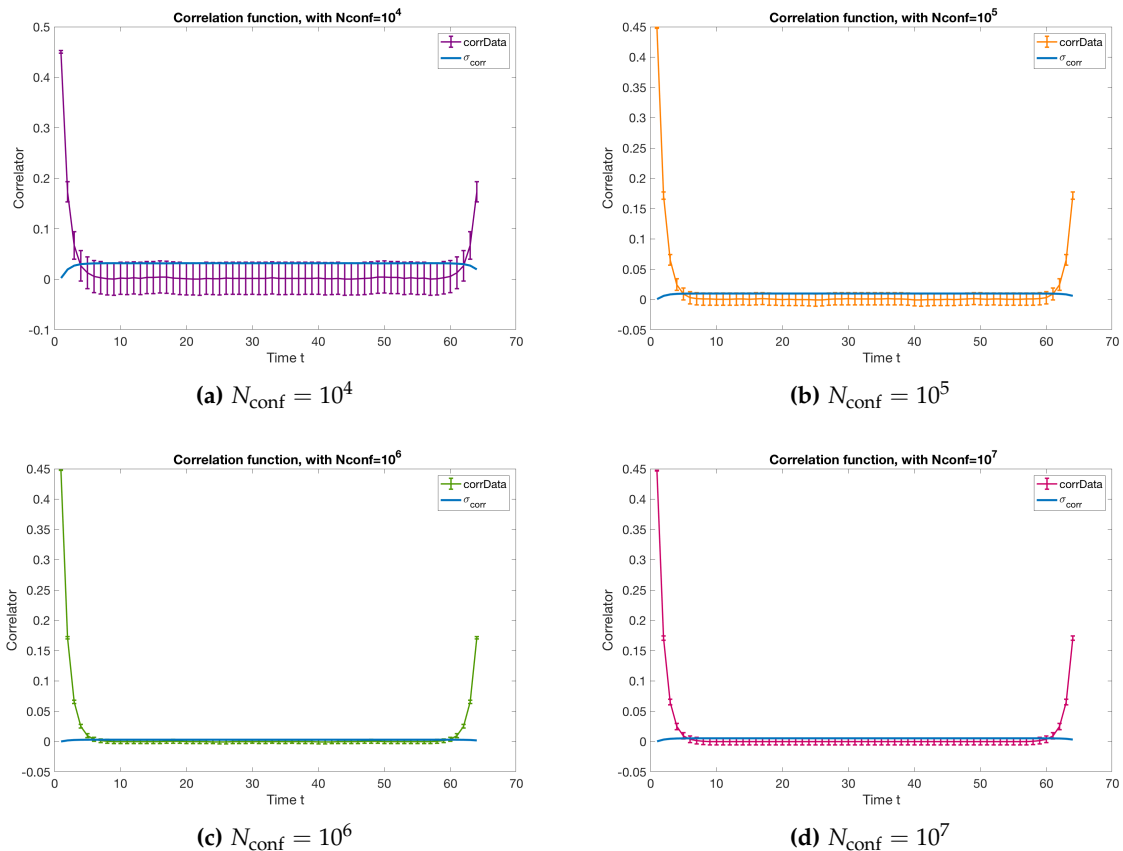


Figure 5: Correlation function averaged over different N_{conf} samples, plotted together with the error line

III. $\Delta\epsilon$ AND MATRIX ELEMENT: RESULTS VS THEORETICAL PREDICTIONS

We have seen that given the correlator data, averaged over the configuration sample, we can calculate $\Delta\epsilon(t)$ and $|\langle\epsilon_0|\hat{x}|\epsilon_1\rangle|(t)$, as in (38) and (39). In our calculations we have chosen $t = 3$ and we have varied⁸ the time lattice spacing a , with fixed $N_{\text{conf}} = 10^6$, ($D_{\text{bin}} = 50$). We can see the results plotted in figures (6) and (7).

Remember from (15) that the eigenvalues of the transfer operator coincide with those of the retarded propagator only in the continuum limit. We can associate to the transfer operator eigenstates and eigenvalues (14) two auxiliary hamiltonians, given by

$$\hat{H} = \frac{\hat{p}^2}{2m} + \frac{1}{2}m\bar{\omega}^2\hat{x}^2$$

which we already defined in (13) and

$$\hat{H} = \frac{\hat{p}^2}{2m} + \frac{1}{2}m\bar{\omega}^2\hat{x}^2$$

⁸The a values were taken so that the product aN was constant and equal to 64. Therefore N values have been changed in accordance

These are related to the original hamiltonian (31) by

$$\epsilon_n = \tilde{\omega} \left(n + \frac{1}{2} \right) \quad (42)$$

$$a\tilde{\omega} = \log \left(1 + a\bar{\omega} + \frac{a^2\omega^2}{2} \right) \quad (43)$$

$$\bar{\omega}^2 = \omega^2 \left(1 + \frac{a^2\omega^2}{4} \right) \quad (44)$$

Then it is easily derived that

$$\Delta\epsilon = \epsilon_1 - \epsilon_0 = \tilde{\omega}(\omega) \quad (45)$$

and

$$|\langle \epsilon_0 | \hat{x} | \epsilon_1 \rangle| = \frac{1}{\sqrt{2\tilde{\omega}}}, \quad m = 1 \quad (46)$$

From (42), (43) and (44) we can derive⁹ the dependence of $\Delta\epsilon$ and $|\langle \epsilon_0 | \hat{x} | \epsilon_1 \rangle|$ on a^2

$$\Delta\epsilon = \omega - \frac{1}{24}a^2\omega^3; \quad |\langle \epsilon_0 | \hat{x} | \epsilon_1 \rangle| = \frac{1}{\sqrt{2\omega}} \left(1 - \frac{a^2}{16}\omega^2 \right), \quad \text{with } \omega = 1$$

The calculated intercept is in accordance with the theoretical predictions.

$$\Delta\epsilon = (1.000 \pm 0.001); \quad |\langle \epsilon_0 | \hat{x} | \epsilon_1 \rangle| = (0.7073 \pm 0.0002)$$

For the $\Delta\epsilon$ value, in the continuum limit¹⁰, the obtained value is in agreement with the prediction within 0.07σ . For the $|\langle \epsilon_0 | \hat{x} | \epsilon_1 \rangle|$ value the agreement is within 1.5σ .

⁹The dependence on a^2 is derived Taylor expanding (45) and (46).

$$\begin{aligned} \Delta\epsilon &= \frac{1}{a} \log \left[1 + a\omega \sqrt{1 + \frac{a^2\omega^2}{4}} + \frac{a^2\omega^2}{2} \right] \sim \frac{1}{a} \log \left[1 + a\omega \left(1 + \frac{1}{8}a^2\omega^2 \right) + \frac{a^2\omega^2}{2} \right] \\ &\sim \frac{1}{a} \left(a\omega + \frac{1}{8}a^3\omega^3 + \frac{1}{2}a^2\omega^2 - \frac{1}{2} \left(a\omega + \frac{1}{8}a^3\omega^3 + \frac{1}{2}a^2\omega^2 \right)^2 + \frac{1}{3} \left(a\omega + \frac{1}{8}a^3\omega^3 + \frac{1}{2}a^2\omega^2 \right)^3 + \dots \right) \\ &= \frac{1}{a} \left(a\omega - \frac{1}{24}a^3\omega^3 + \dots \right) \sim \omega - \frac{1}{24}a^2\omega^2 \sim 1 - (0.0417)a^2 \end{aligned}$$

$$\begin{aligned} |\langle \epsilon_0 | \hat{x} | \epsilon_1 \rangle| &= \frac{1}{\sqrt{2\sqrt{\omega^2 \left(1 + \frac{a^2\omega^2}{4} \right)}}} \sim \frac{1}{\sqrt{2\omega}} \frac{1}{\sqrt{1 + \frac{a^2\omega^2}{8}}} \\ &\sim \frac{1}{\sqrt{2\omega}} \left(1 - \frac{a^2\omega^2}{16} \right) \sim 0.707 - (0.0442)a^2 \end{aligned}$$

¹⁰When we send $a \rightarrow 0$ we into account a significant increase in computation time.

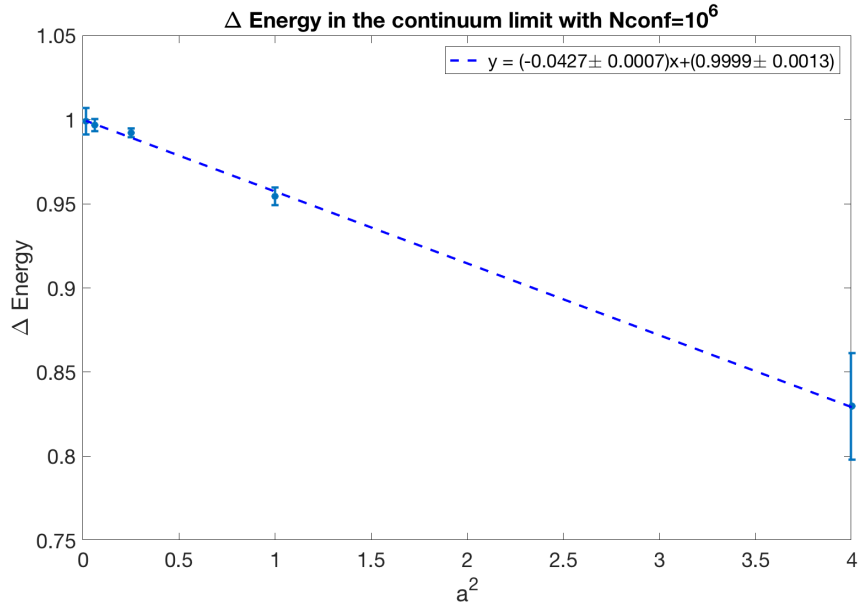


Figure 6: $\Delta \epsilon$, for $t = 3$, plotted against lattice spacing a^2 . We notice the as a becomes smaller the values approach the theoretical prediction.

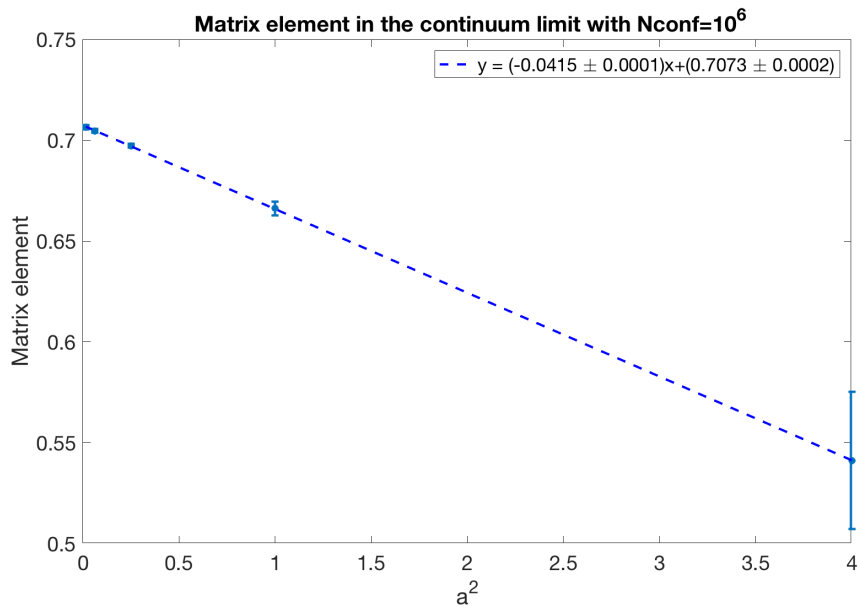


Figure 7: $|\langle \epsilon_0 | \hat{x} | \epsilon_1 \rangle|$, for $t = 3$, plotted against lattice spacing a^2 . We notice the as a becomes smaller the values approach the theoretical prediction.

IV. HAMILTONIAN MONTE CARLO (HMC): $\lambda\phi^4$ THEORY

I. SCALAR $\lambda\phi^4$ THEORY ON LATTICE IN 3-D

In the second part of the project we implement a scalar lattice field theory $\lambda\phi^4$. The continuous version of the Lagrangian of the system, in the Euclidean time formalism, is given by

$$\mathcal{L} = \frac{1}{2}\partial_\mu\phi\partial^\mu\phi + \frac{1}{2}m^2\phi^2 + \frac{\lambda}{4!}\phi^4 \quad (47)$$

so that the action is

$$\mathcal{S} = \int d^4x \mathcal{L}(\phi, \partial_\mu\phi)$$

The discretized version of the action is

$$\mathcal{S}(\phi) = \sum_{x \in \Lambda} \left[-2k \left\{ \sum_{\eta=0}^{D-1} \phi(x)\phi(x+\eta) \right\} + \phi^2(x) + \lambda(\phi^2(x) - 1)^2 \right] \quad (48)$$

where x denote the lattice sites, referred to as Λ . We define the model on a D dimensional lattice with lattice spacing a (from now on a is set to 1). The real valued field ϕ lives on the sites and we adopt periodic boundary conditions, i.e. if μ is the unit vector in the μ direction, then

$$\phi(x + L\mu) = \phi(x)$$

The constant values that appear in (48) are set as $\lambda = 1.3282$ and $k = 0.18169$, if not otherwise indicated.

All the parameters of the lattice, the dimension D (which is fixed to 3), the spatial extent L and the volume V , are defined in *lattice.h*.

II. HAMILTONIAN MONTE CARLO (HMC)

As in the case of the harmonic oscillator, the calculation of the observables is linked to the path integral formalism. In fact, the expectation value of an operator $\langle \hat{O} \rangle$ is given by

$$\langle \hat{O} \rangle = \frac{1}{Z} \int [\mathcal{D}\phi] \hat{O}(\phi) e^{-\mathcal{S}} \quad (49)$$

in analogy with (29), where the trajectories $[Dx]$ have become field configurations $[\mathcal{D}\phi]$, Z is the system partition function

$$Z \equiv \int [\mathcal{D}\phi] e^{-\mathcal{S}}$$

and \mathcal{S} is given in (47).

If there were an algorithm that extracted field configurations according to probability distribution $P_S(\phi) = \frac{1}{Z} e^{-\mathcal{S}}$, then we would be able to calculate observables averaged over the generated sample as

$$\bar{O} \equiv \frac{1}{N_{\text{nconf}}} \sum_{i=1}^{N_{\text{nconf}}} O(\phi_i)$$

In the previous part we implemented the Metropolis algorithm, but, in the case of $\lambda\phi^4$ theory, it becomes inefficient since local updates, as those used for the harmonic oscillator, explore the configuration space slowly, i.e. there are long autocorrelations. Moreover, since the action is extensive, even if we simultaneously updated the field, the difference between the initial and the final action, ΔS , would be considerable and the acceptance rate would be low.

In order to bypass these problems, we use a different algorithm, which involves parallel updates of the field at all lattice sites, followed by an accept/reject step that decides for the whole configuration. The algorithm is known as Hamiltonian Monte Carlo (HMC). It introduces a new parameter τ , called simulation time, and makes use of the hamiltonian dynamics equations to evolve the field ϕ over τ .

To implement the HMC algorithm, we introduce an auxiliary field π , so that the new Hamiltonian becomes

$$H(\phi, \pi) = \frac{1}{2} \sum_{x \in \Lambda} \pi^2(x) + \mathcal{S}(\phi) \quad (50)$$

The partition function Z now depends on π

$$Z_H = \int [\mathcal{D}\phi] [\mathcal{D}\pi] e^{-H(\phi, \pi)} \quad (51)$$

and the two fields, ϕ and π , both acquire dependence on τ

$$\pi(x) \rightarrow \pi(x, \tau), \quad \phi(x) \rightarrow \phi(x, \tau)$$

We can interpret $\pi(x, \tau)$ as the conjugate momenta of $\phi(x, \tau)$ as obtained from (50).

The two fields, $\pi(x, \tau)$ and $\phi(x, \tau)$, satisfy the Hamilton equations, called Molecular Dynamics equations, (MD equations)

$$\begin{aligned} \frac{d\phi(x, \tau)}{d\tau} &= \frac{\partial \mathcal{H}(\phi, \pi)}{\partial \pi(x, \tau)} = \pi(x, \tau) \\ \frac{d\pi(x, \tau)}{d\tau} &= -\frac{\partial \mathcal{H}(\phi, \pi)}{\partial \phi(x, \tau)} = -\frac{\delta \mathcal{S}(\phi)}{\delta \phi(x, \tau)} \equiv -F(x, \tau) \end{aligned} \quad (52)$$

The introduction of the auxiliary π field makes possible to generate field configurations based on (52). These are equations of motions for the artificial hamiltonian and from their solution we can construct a valid update algorithm, since they conserve the hamiltonian and the phase space volume (Liouville's theorem). In other words a configuration of (ϕ, π) is equally likely to the (ϕ', π') , which is obtainable using (ϕ, π) as initial condition and solving the equations of motions for some time τ .

The HMC algorithm would be ideal if we were able to solve the equations of motion exactly. In general, we solve them using some numerical method, as the leapfrog integrator in our case, and integration errors occur.

However it becomes exact if we add a Metropolis step at the end of each trajectory. We call it the accept/reject step. This procedure works if two requirements are satisfied: time-reversibility and conservation of the phase space volume.

Here we outline the scheme of the HMC algorithm:

1. Start with a random configuration of the ϕ field $\phi_0(x, \tau)$.
2. Sample a random initial momenta configuration $\pi_0(x, \tau)$, according to a gaussian distribution of zero mean and unit variance.

$$P_G(\pi) = \frac{e^{\frac{1}{2} \sum_{x \in \Lambda} \pi^2(x)}}{\int [d\pi] e^{\frac{1}{2} \sum_{x \in \Lambda} \pi^2(x)}} = \frac{e^{\frac{1}{2} \sum_{x \in \Lambda} \pi^2(x)}}{Z_\pi}$$

3. Numerically solve the hamiltonian equations of motions (52) for some τ_0 (in our case $\tau_0 = 1$). This moves (ϕ, π) to a new proposed configuration (ϕ', π') . Note that the proposal is deterministic, since the probability to go to (ϕ', π') is different from zero only if the new field is a solution of the MD equations.

$$P_{MD}((\phi, \pi) \rightarrow (\phi', \pi')) = \delta(\phi' - \phi)\delta(\pi' - \pi)$$

4. Calculate the change in the hamiltonian

$$\Delta H = H(\phi', \pi') - H(\phi, \pi)$$

5. Accept the proposed configuration ϕ' with probability

$$P_A((\phi, \pi) \rightarrow (\phi', \pi')) = \min\{1, e^{-\Delta H}\}$$

6. Otherwise $\phi' = \phi$

The algorithm updates the ϕ field with probabiity

$$P_M(\phi \rightarrow \phi') = \int [\mathcal{D}\pi] [\mathcal{D}\pi'] P_G(\pi) P_{MD}((\phi, \pi) \rightarrow (\phi', \pi')) P_A((\phi, \pi) \rightarrow (\phi', \pi'))$$

We can show that this assures that the detailed balanced condition¹¹

$$P_M(\phi \rightarrow \phi') P_S(\phi) = P_M(\phi' \rightarrow \phi) P_S(\phi')$$

¹¹ To prove that the detailed balance condition is guaranteed, we need the following results:

1. $P_S(\phi) P_G(\pi) = \frac{1}{Z_H} e^{-H(\phi, \pi)}$
2. $P_{MD}((\phi, \pi) \rightarrow (\phi', \pi')) = P_{MD}((\phi', -\pi') \rightarrow (\phi, -\pi))$, since the leapfrog integrator is area preserving.
3. $P_S(\phi) P_G(\pi) P_A((\phi, \pi) \rightarrow (\phi', \pi')) = P_S(\phi') P_G(\pi') P_A((\phi', \pi') \rightarrow (\phi, \pi))$, which follows from the first two

Proof.

$$\begin{aligned} P_S(\phi) P_M(\phi \rightarrow \phi') &= \int [\mathcal{D}\pi] [\mathcal{D}\pi'] P_S(\phi) P_G(\pi) P_{MD}((\phi, \pi) \rightarrow (\phi', \pi')) P_A((\phi, \pi) \rightarrow (\phi', \pi')) \\ &\stackrel{2,3)}{=} \int [\mathcal{D}\pi] [\mathcal{D}\pi'] P_S(\phi') P_G(-\pi') P_{MD}((\phi', -\pi') \rightarrow (\phi, -\pi)) P_A((\phi', -\pi') \rightarrow (\phi, -\pi)) \\ &= \int [\mathcal{D}\pi] [\mathcal{D}\pi'] P_S(\phi') P_G(\pi') P_{MD}((\phi', \pi') \rightarrow (\phi, \pi)) P_A((\phi', \pi') \rightarrow (\phi, \pi)) \\ &= P_S(\phi') P_M(\phi' \rightarrow \phi) \end{aligned}$$

where in last passage we renamed $\pi \rightarrow -\pi$ and $\pi' \rightarrow -\pi'$. □

is satisfied and so that the trajectories will follow P_S for large N_{conf} . We run the program for $N_{\text{term}} = 10^3$ times to thermalize the trajectories. We have always used $N_{\text{conf}} = 10^6$. Finally, as in the harmonic oscillator part, in order to have uncorrelated data, we perform the binning procedure on the trajectories, with $N_{\text{bin}} = 10^3$. The acceptance rate is always maintained over 70%.

In the following sections we enter in detail of each step of the algorithm.

ii.1 Sampling random momenta π

The conjugate momenta are to be generated following a Gaussian distribution. In order to do so, we use a random number generator routine *ranlxd.c* by Martin Luescher, which extracts with flat distribution. Then we use the Box-Muller procedure to convert x_1, x_2 , flatly distributed numbers, to y_1, y_2 , which are distributed according to P_G

$$\begin{aligned} y_1 &= \sqrt{-2 \ln(1 - x_1)} \cos(2\pi(1 - x_2)) \\ y_2 &= \sqrt{-2 \ln(1 - x_1)} \sin(2\pi(1 - x_2)) \end{aligned}$$

ii.2 Discrete MD integrator: Leapfrog

The Markovian time τ_0 is divided into $nstep$ parts ($nstep$ is a changeable parameter) in $\delta\tau = \frac{\tau_0}{nstep}$. Then we use Taylor expansion to update firstly the ϕ field, the π field and then ϕ again

$$\begin{aligned} \phi(\tau + \delta\tau) &= \phi(\tau) + \delta\tau\dot{\phi}(\tau) + o(\delta\tau^2) \\ \pi(\tau + \delta\tau) &= \pi(\tau) + \delta\tau\dot{\pi}(\tau) + o(\delta\tau^2) \end{aligned}$$

Since

$$\dot{\phi}(\tau) = \frac{\delta H}{\delta \pi} = \pi(\tau) \quad \dot{\pi}(\tau) = -\frac{\delta H}{\delta \phi} = -\frac{\delta \mathcal{S}}{\delta \phi} = -F(\tau)$$

with $F(\tau) = -2k \sum_{\eta=0}^{D-1} [\phi(x + \eta) + \phi(x - \eta)]$, the two fields can be updated independently according to

$$\begin{bmatrix} \phi(\tau + \delta\tau) \\ \pi(\tau) \end{bmatrix} = I_\phi(\delta\tau) \begin{bmatrix} \phi(\tau) \\ \pi(\tau) \end{bmatrix} = \begin{bmatrix} \mathbb{1} & \delta\tau \\ 0 & \mathbb{1} \end{bmatrix} \begin{bmatrix} \phi(\tau) \\ \pi(\tau) \end{bmatrix} \quad (53)$$

$$\begin{bmatrix} \phi(\tau) \\ \pi(\tau + \delta\tau) \end{bmatrix} = I_\pi(\delta\tau) \begin{bmatrix} \phi(\tau) \\ \pi(\tau) \end{bmatrix} = \begin{bmatrix} \mathbb{1} & 0 \\ -\delta\tau \frac{F(\tau)}{\phi(\tau)} & \mathbb{1} \end{bmatrix} \begin{bmatrix} \phi(\tau) \\ \pi(\tau) \end{bmatrix} \quad (54)$$

The leapfrog integrator is the following combination of (53) and (54)

$$I_{LPF}(\delta\tau) = I_\pi \left(\frac{\delta\tau}{2} \right) I_\phi(\delta\tau) I_\pi \left(\frac{\delta\tau}{2} \right) \quad (55)$$

Then

$$I_{LPF}(\tau_0) = [I_{LPF}(\delta\tau)]^{nstep}$$

This integrator satisfies the two requirements, discussed before, for the algorithm to be exact: time-reversibility (note the symmetric form of (55)) and area-preserving property.

ii.3 Time-Reversibility and Area-Preserving

Time-reversibility means that if we perform one trajectory $((\phi, \pi) \rightarrow (\phi', \pi'))$, then flip the momentum sign $\pi' \rightarrow -\pi'$ and use the same algorithm to run the trajectory back to $((\phi', -\pi') \rightarrow (\phi'', \pi''))$, we end up at the starting point ($\phi'' = \phi$). We have checked this property for different $nstep$ values and always obtained results compatible with the computer rounding errors, as one can see from the table below

$nstep$	$ \phi'' - \phi $
10	7.97e-17
15	8.57e-17
20	7.44e-17
25	1.10e-16
30	1.01e-16

On the other hand, a consequence of the phase space area-preserving property is that the exponential of the change in the hamiltonian ΔH is on average one

$$\langle e^{-\Delta H(\phi, \pi)} \rangle = \frac{1}{Z_H} \int [\mathcal{D}\phi] [\mathcal{D}\pi] e^{-H(\phi, \pi)} e^{-\Delta H(\phi, \pi)} = \frac{1}{Z_H} \int [\mathcal{D}\phi_0] [\mathcal{D}\pi_0] e^{-H(\phi_0, \pi_0)} = 1$$

This can be verified in the following table

$nstep$	$\langle e^{-\Delta H(\phi, \pi)} \rangle$
10	0.9935 \pm 0.0001
15	0.99871 \pm 0.00005
20	0.99962 \pm 0.00003
25	0.99981 \pm 0.00002
30	0.99992 \pm 0.00001

The results become more accurate as $nstep$ increases, since $\delta\tau$ becomes smaller.

ii.4 The hamiltonian is not conserved

Since the MD equations cannot be solved exactly, but a numeric integrator has to be implemented, the hamiltonian is not conserved exactly either. It is in the limit $\delta\tau \rightarrow 0$, that we are approaching the ideal case. We expect that $|\Delta H|$ approaches zero linearly with $\delta\tau^2$, as we can see in figure (8)

ii.5 The accept/reject step

Figure (9) illustrates the difference between an algorithm that implements the accept/reject step and a one that does not. $\langle m^2 \rangle / V^2$, (where $V = L^D$), is plotted against $\delta\tau^2$. In the case of the accept/reject step the value of the observable is independent of $\delta\tau^2$ (the angular coefficient of the interpolating linear function is zero within 1.5σ). In fact, adding a

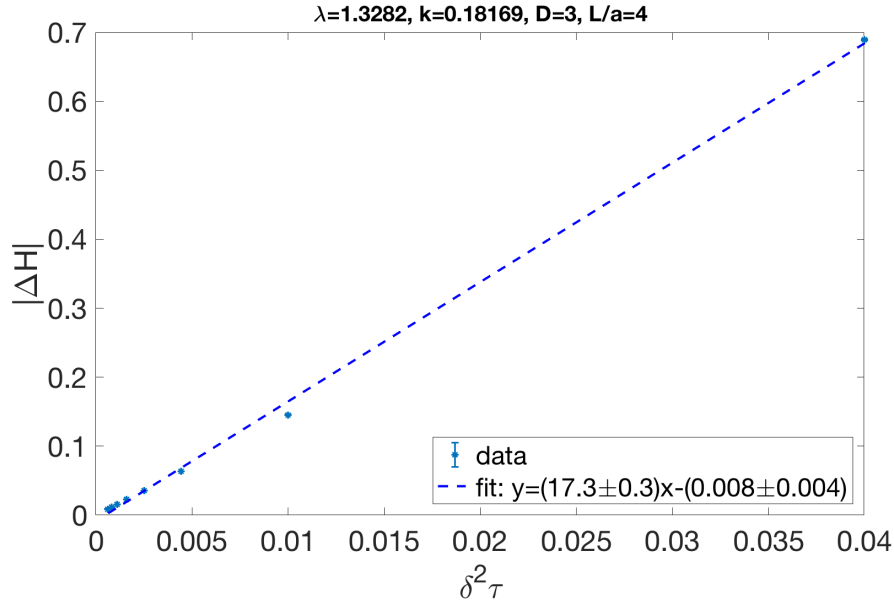


Figure 8: ΔH values calculated without the accept/reject step are plotted against $\delta\tau^2$; a linear interpolation is observed

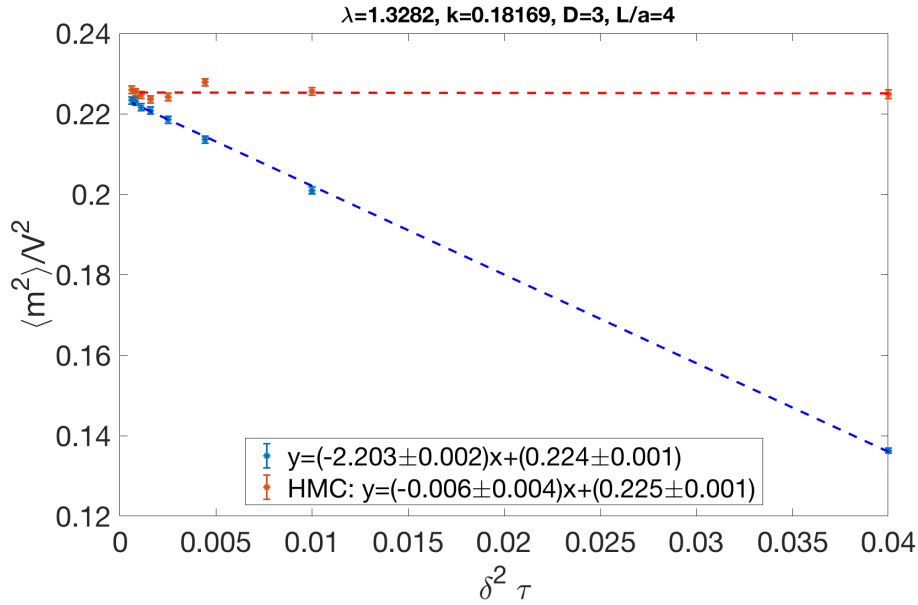


Figure 9: $\langle m^2 \rangle / V^2$ is plotted against $\delta\tau^2$ with and without the accept/reject step

Metropolis step at the end of each trajectory makes the algorithm correct for each value of $\delta\tau^2$, even if the hamiltonian is not exactly conserved.

On the other side, without the accept/reject step, the algorithm is correct only in the

limit $\Delta H \rightarrow 0$, i.e. in the ideal case where $\delta\tau^2$ is infinitesimal.

The figure (9) also shows that the two plots have the same y intercept, confirming our predictions.

III. SPONTANEOUS SYMMETRY BREAKING

Once we have a valid algorithm, we perform a study of the spontaneous symmetry breaking in $\lambda\phi^4$ theory. Data are collected once thermalization is done and the binning procedure is implemented in order to uncorrelate data. We'll work with a fixed value of $\lambda = 1.145$ and will vary the k values, with k in $[0.15, 0.21]$. We will see that spontaneous symmetry breaking occurs for $0.18 < \tilde{k} < 0.19$. We are looking at few observables, which are functions of the magnetization m , considered as a primary variable:

$$m = \sum_{x \in \Lambda} \phi(x) \quad (56)$$

The following quantities are studied:

-

$$\frac{\langle m^2 \rangle}{V^2} \quad (57)$$

- *magnetic susceptibility* χ :

$$\chi = \frac{[\langle m^2 \rangle - \langle |m| \rangle^2]}{V} \quad (58)$$

- *Binder cumulant* U :

$$U = \frac{\langle m^4 \rangle}{(\langle m^2 \rangle)^2} \quad (59)$$

Their evolution against k values is plotted in figures (10), (11) and (12). We can notice that the three observables, when $0.18 < \tilde{k} < 0.19$, change suddenly, signaling that symmetry breaking has occurred.

For great k , $\langle m^2 \rangle / V^2$ seems to be independent of L . This indicates that we are in the broken symmetry phase. Moreover, it suddenly passes from zero values to non-zero ones when \tilde{k} is approached.

This happens for the susceptibility as well, since far from the pick, where is the transition, χ values no longer depend on L .

For the Binder cumulant, instead, we can see that at the critical point, \tilde{k} , the observable is independent the lattice size.

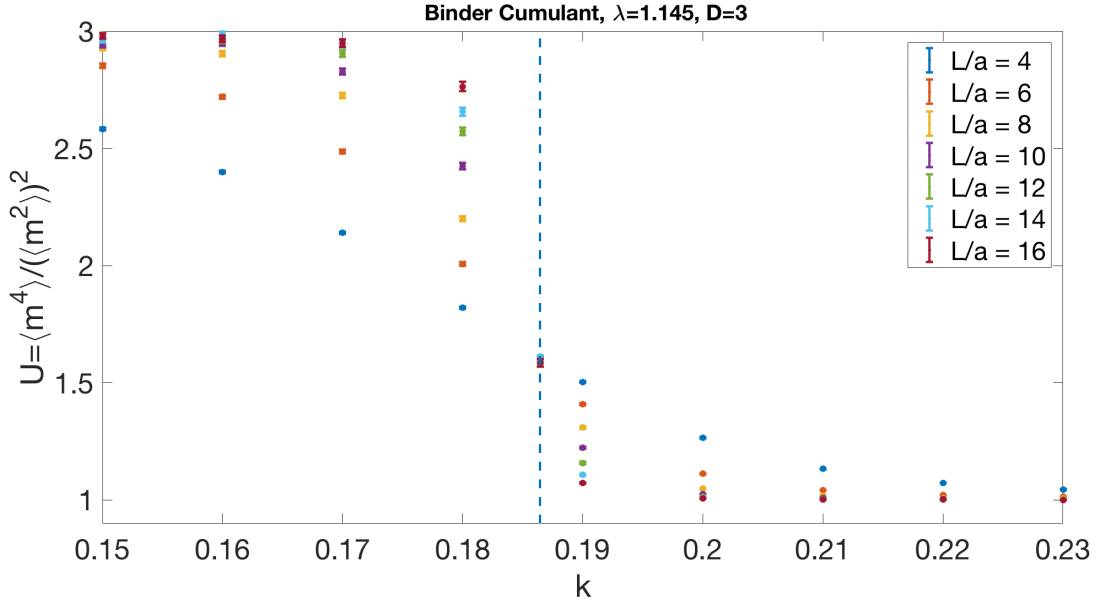


Figure 10: Binder Cumulant vs k : at the critical value of k , marked with a blue vertical line, the values are independent of the lattice size signaling a symmetry breaking.

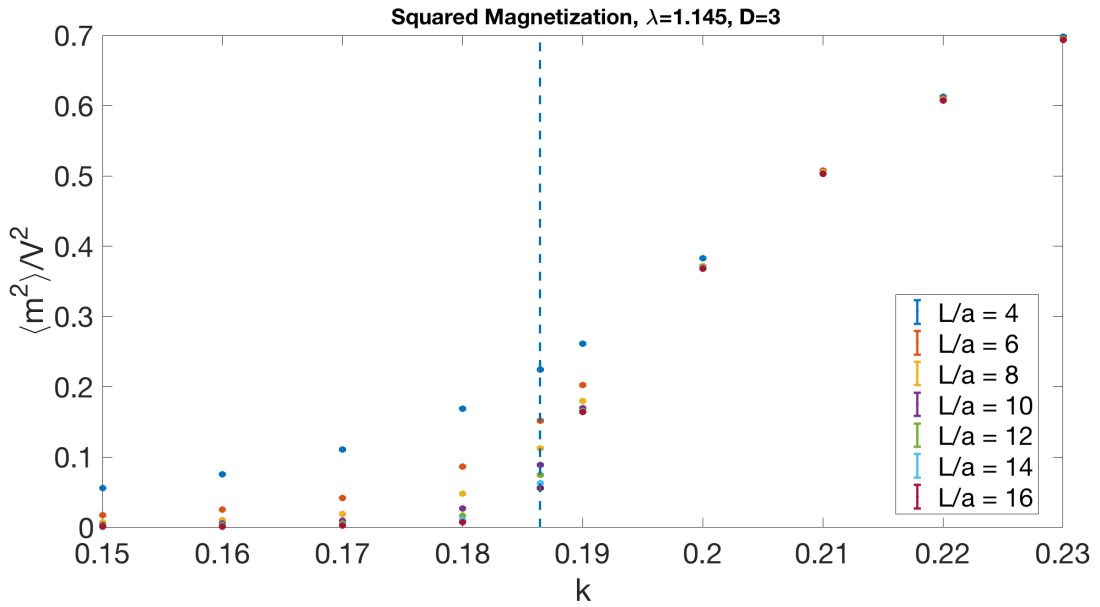


Figure 11: $\frac{\langle m^2 \rangle}{N^2}$ vs k : after the critical point, marked with a vertical blue line, the observable assumes definitely a non zero value and becomes independent of L .

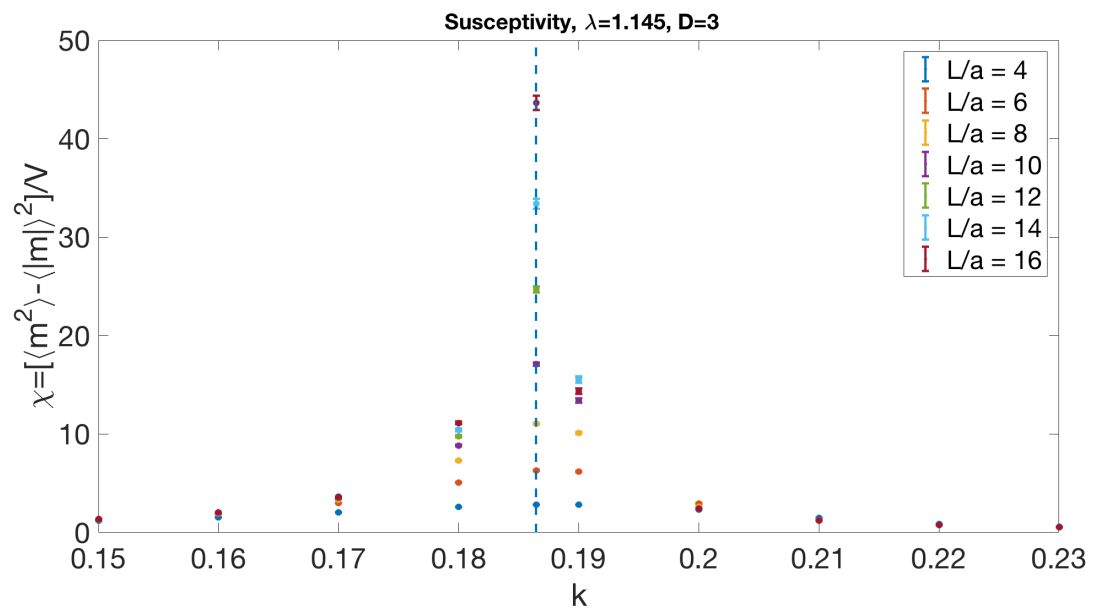


Figure 12: Susceptibility vs k : far from the critical point, marked with a vertical blue line, the observable is no longer dependent on L

A. JACKKNIFE METHOD FOR ERROR ANALYSIS

The jackknife procedure is a useful resampling technique which we used for the standard deviation estimation, when dealing with non primary variables. It allows to avoid all the derivative part calculations as would be in the standard procedure of uncertainty propagation. Here we illustrate how the method works.

Consider a single observable. It is a random variable with its associated expectation value

$$\langle a \rangle = \int da [aP(a)], \quad \text{VAR}(a) = \langle (a - \langle a \rangle)^2 \rangle$$

Suppose now that we have N independent values of this variable. Then the best estimate for this observable is its mean over the sample given by

$$\bar{a} = \frac{1}{N} \sum_{i=0}^{N-1} a_i$$

with the associated error given by

$$\sigma_{\bar{a}} = \frac{1}{\sqrt{N}} \sqrt{\frac{\sum_{i=0}^{N-1} (a_i - \bar{a})^2}{N-1}}$$

This is standard statistic estimations and all works well as long as we have to deal with a primary variable as a , of which we have independent measures.

Suppose now that we have a function of the expectation value of a , $f(\langle a \rangle)$. Its mean and relative uncertainty can be derived using standard error propagation techniques which involve derivatives, not always easy to perform

$$\bar{f} = f(\bar{a}) = f + \left. \frac{\partial f}{\partial a} \right|_{a=\langle a \rangle} \langle \bar{a} - \langle a \rangle \rangle + o\left(\frac{1}{N}\right)$$

$$\sigma_{\bar{f}}^2 = \left(\left. \frac{\partial f}{\partial a} \right|_{a=\langle a \rangle} \right)^2 \sigma_{\bar{a}}^2$$

Here comes the Jackknife method. Given our N configurations of the primary variable a , we define the clusterized data as follows

$$a^k \equiv \frac{1}{N-1} \left[\sum_{i=0}^{N-1} a_i - a_k \right] = \bar{a} - \frac{(a_k - \bar{a})}{N-1} \quad (60)$$

where k goes from 0 to $N-1$. We note that the a^k values are more stable than the original values of the random variable, since the possible oscillations around the mean are suppressed by the factor $1/(N-1)$.

We can now define the mean and the variance for the clusterized values of the primary variable a

$$[\bar{a}]_j \equiv \frac{1}{N} \sum_{k=0}^{N-1} a^k = \bar{a} \quad (61)$$

$$[\sigma^2(\bar{a})]_j \equiv \frac{N-1}{N} \sum_{k=0}^{N-1} (a^k - \bar{a})^2 = \sigma^2(\bar{a}) \quad (62)$$

where the subscript j indicates that we followed the jackknife procedure.

In a similar way, we clusterize the composite variables given by $f(\langle a \rangle)$:

$$f^k = f(a^k)$$

Then the uncertainty on the mean value \bar{f} can be simply calculated, avoiding the derivatives as

$$\sigma_j^2(\bar{f}) = \frac{N-1}{N} \sum_{k=0}^{N-1} (f^k - \bar{f})^2 \quad (63)$$

We can show that (63) is an unbiased estimator of the variance of the sample mean

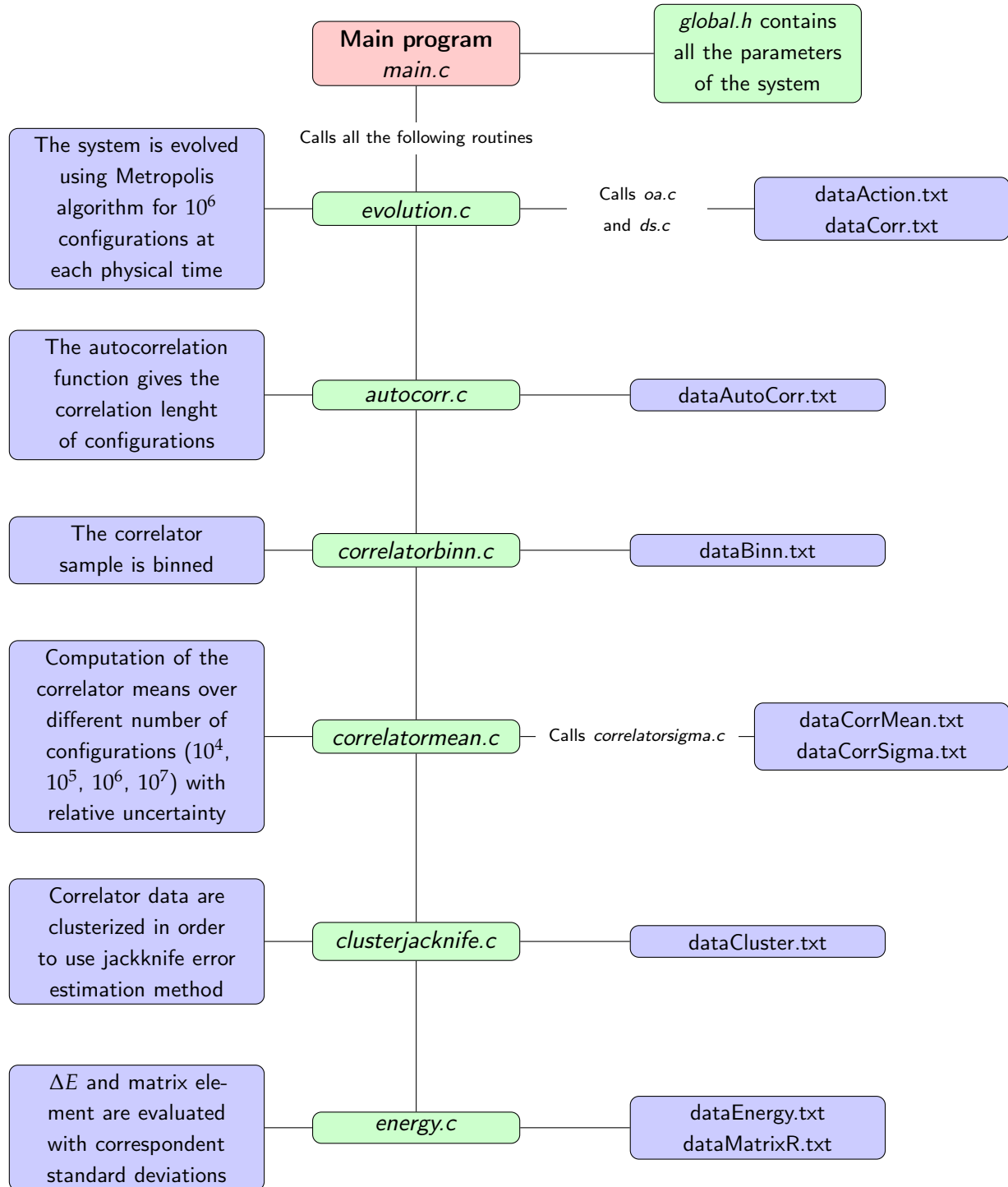
$$\begin{aligned} f^k &= f\left(\bar{a} - \frac{(a_k - \bar{a})}{N-1}\right) = \bar{f} - \left.\frac{\partial f}{\partial a}\right|_{a=\langle a \rangle} \frac{(a_k - \bar{a})}{N-1} + \dots + o(1/N) \\ \sigma_j^2(\bar{f}) &= \frac{N-1}{N} \sum_{k=0}^{N-1} \left[\left.\frac{\partial f}{\partial a}\right|_{a=\langle a \rangle} \frac{(a_k - \bar{a})}{N-1}\right]^2 = \\ &= \frac{N-1}{N} \frac{1}{(N-1)^2} \left(\left.\frac{\partial f}{\partial a}\right|_{a=\langle a \rangle}\right)^2 \sum_{k=0}^{N-1} (a_k - \bar{a})^2 = \\ &= \frac{1}{N(N-1)} \left(\left.\frac{\partial f}{\partial a}\right|_{a=\langle a \rangle}\right)^2 \sum_{k=0}^{N-1} (a_k - \bar{a})^2 = \\ &= \left(\left.\frac{\partial f}{\partial a}\right|_{a=\langle a \rangle}\right)^2 \frac{\sigma^2(a)}{N} = \\ &= \left(\left.\frac{\partial f}{\partial a}\right|_{a=\langle a \rangle}\right)^2 \sigma^2(\bar{a}) \end{aligned}$$

As a final remark, we have to take into account that if (61) holds for the primary variables, there is a bias if we are working with composite variables

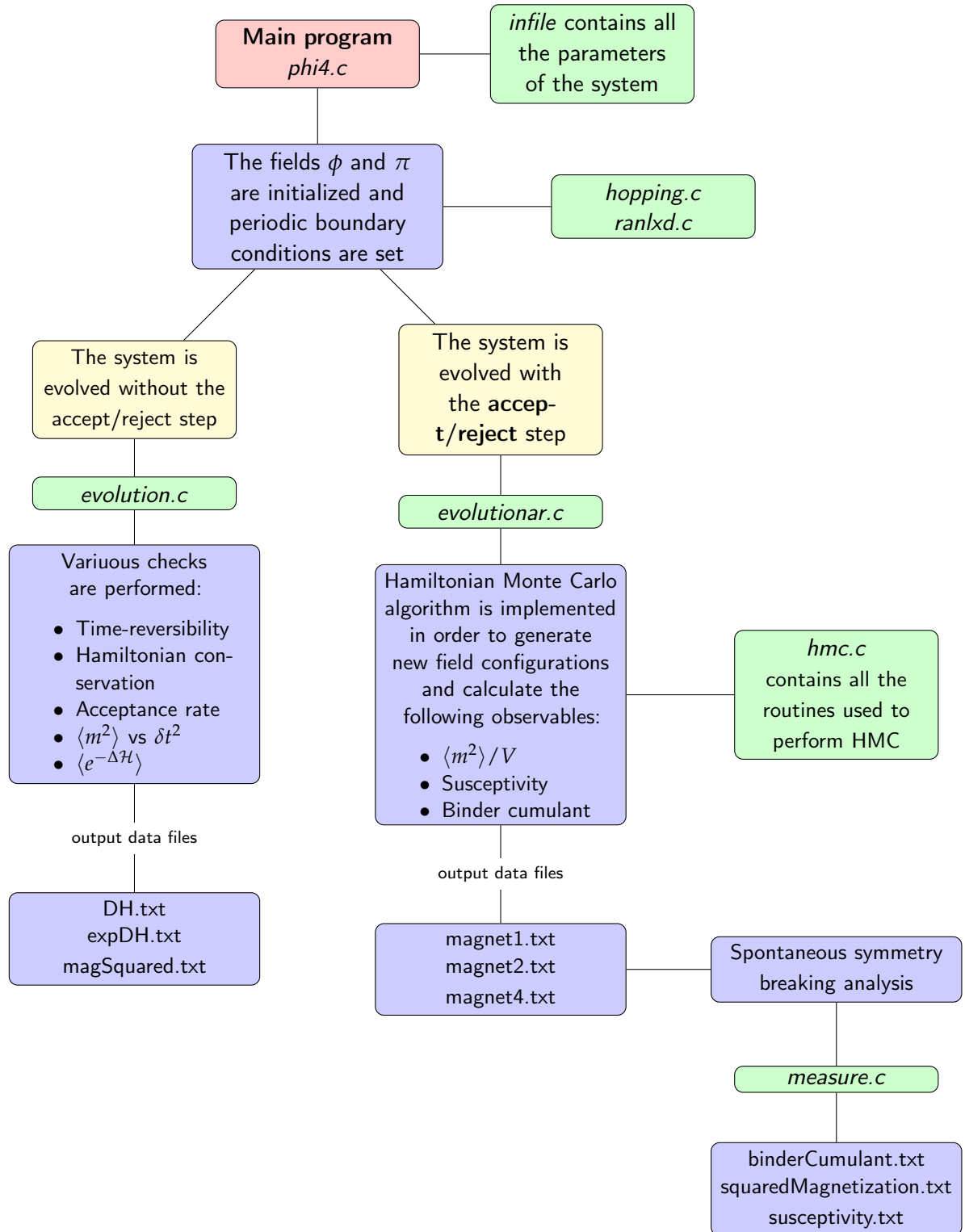
$$\bar{f} \neq \frac{1}{N} \sum_k f^k$$

A. OUTLINE OF THE PROGRAMS

I. HARMONIC OSCILLATOR (LFC18)



II. $\lambda\phi^4$ THEORY (**phi4**)



REFERENCES

REFERENCES

- [1] *Class notes*: notes from lessons by Giusti and Dalla Brida
- [2] A. Barp, F. X. Briol, A. D. Kennedy, M. Girolami. *Geometry and Dynamics for Markov Chain Monte Carlo*, @ <https://arxiv.org/abs/1705.02891>
- [3] S. Duane, A. D. Kennedy, B. J. Pendleton, D. Roweth. Published in Phys. Lett. B195 (1987) 216-222. *Hybrid Monte Carlo*
- [4] Michael Betancourt *A Conceptual Introduction to Hamiltonian Monte Carlo*, @ <https://arxiv.org/abs/1701.02434>